Excitation of large-scale inertial waves in a rotating inhomogeneous turbulence

Tov Elperin,* Ilia Golubev,† Nathan Kleeorin,‡ and Igor Rogachevskii§
The Pearlstone Center for Aeronautical Engineering Studies, Department of Mechanical Engineering, Ben-Gurion University of the Negev, Beer-Sheva 84105, P.O. Box 653, Israel

(Received 3 August 2004; revised manuscript received 11 November 2004; published 14 March 2005)

A mechanism of excitation of the large-scale inertial waves in a rotating inhomogeneous turbulence due to an excitation of a large-scale instability is found. This instability is caused by a combined effect of the inhomogeneity of the turbulence and the uniform mean rotation. The source of the large-scale instability is the energy of the small-scale turbulence. We determined the range of parameters at which the large-scale instability occurs, the growth rate of the instability, and the frequency of the generated large-scale inertial waves.

DOI: 10.1103/PhysRevE.71.036302 PACS number(s): 47.27.−i, 47.35.+i, 47.32.−y

I. INTRODUCTION

The study of rotating flows is of interest for a wide range of problems, ranging from engineering (e.g., turbomachinery) and astrophysics (galactic and accretion disks) to geophysics (oceans, the atmosphere of the Earth, gaseous planets) and weather predictions (see, e.g., [1–3]). Inertial waves arise in rotating flows and are observed in the atmosphere of the Earth and in laboratory rotating flows. In turbulent rotating flows inertial waves are damped due to a high turbulent viscosity. Thus, excitation of coherent and undamped inertial waves by turbulence seems not to be effective. However, large-scale inertial waves are observed in turbulent rotating flows. A mechanism of excitation of the large-scale coherent inertial waves in turbulence is not well understood.

Inertial waves are related to generation of large-scale vorticity. Generation of a large-scale vorticity in a helical turbulence due to hydrodynamical α effect was suggested in [4–8]. This effect is associated with the $\alpha\tilde{\mathbf{W}}$ term in the equation for the mean vorticity, where $\tilde{\mathbf{W}}$ are the perturbations of the mean vorticity and α is determined by the hydrodynamical helicity of turbulent flow. A nonzero hydrodynamical helicity is caused, e.g., by a combined effect of an uniform rotation and inhomogeneity of turbulence (or fluid density stratification).

Formation of large-scale vortices in a turbulent rotating flows was studied experimentally and in numerical simulations (see, e.g., [9–15]). Formation of large-scale coherent structures (e.g., large-scale cyclonic and anticyclonic vortices) in a small-scale turbulence is one of the characteristic features of rotating turbulence (see, e.g., [11]). A number of mechanisms have been proposed to describe generation of a mean flow by a small-scale rotating turbulence—e.g., the effect of angular momentum mixing [16] and vorticity expulsion [17]. The first experimental demonstration wherein it was shown that the divergence of the Reynolds stresses can generate an organized mean circulation was described in [11].

There is a certain similarity between mean rotation and a mean velocity shear. Generation of a mean vorticity in a nonhelical homogeneous incompressible turbulent flow with an imposed mean velocity shear due to an excitation of a large-scale instability was studied in [18]. This instability is caused by a combined effect of the large-scale shear motions ("skew-induced" deflection of equilibrium mean vorticity) and "Reynolds stress-induced" generation of perturbations of the mean vorticity. This instability and the dynamics of the mean vorticity are associated with Prandtl's turbulent secondary flows (see, e.g., [19–22]). However, a turbulence with an imposed mean velocity shear and a uniformly rotating turbulence are different. In particular, the mean vorticity is generated by a homogeneous nonhelical sheared turbulence [18]. On the other hand, the mean vorticity cannot be generated by a homogeneous uniformly rotating nonhelical turbulence (see below). The main difference between these two flows is that the mean velocity shear produces work in a turbulent flow, while a uniform rotation does not produce work in a homogeneous turbulent flow.

There are other interesting problems related with the inertial waves including, e.g., the effect of inertial waves on the onset of convection and on the turbulence dynamics. In particular, the onset of convection in the form of inertial waves in a rotating fluid sphere were studied in [23]. On the other hand, the modification of turbulence dynamics by rotation is due to the presence of small-scale inertial waves in rotating flows (see, e.g., [2,24–27]).

The main goal of this paper is to study large-scale structures formed in a rotating inhomogeneous turbulence. In particular, we investigate the excitation of large-scale inertial waves. These structures are associated with a generation of a large-scale vorticity due to the excitation of the large-scale instability in an uniformly rotating inhomogeneous turbulence. The excitation of the mean vorticity in this system requires an inhomogeneity of turbulence.

This paper is organized as follows. In Sec. II we formulated the governing equations, the assumptions, and the procedure of the derivation. In Sec. III the effective force was determined, which allowed us to derive the mean-field equations and to study the excitation of large-scale inertial waves

*Electronic address: elperin@menix.bgu.ac.il; URL: http://www.bgu.ac.il/~elperin
†Electronic address: golubev@bgumail.bgu.ac.il
‡Electronic address: nat@menix.bgu.ac.il
§Electronic address: gary@menix.bgu.ac.il; URL: http://www.bgu.ac.il/~gary

in Sec. IV. The large-scale instability was investigated in Sec. IV analytically for a weakly inhomogeneous turbulence and numerically for an arbitrary inhomogeneous turbulence. Conclusions and applications of the obtained results are discussed in Sec. V. In Appendixes A–C a detailed derivation of the effective force is performed.

II. GOVERNING EQUATIONS

The system of equations for the evolution of the velocity $\mathbf{v}$ and vorticity $\mathbf{W} \equiv \boldsymbol{\nabla} \times \mathbf{v}$ reads

$$\left[\frac{\partial}{\partial t} + \mathbf{v} \cdot \boldsymbol{\nabla}\right]\mathbf{v} = -\frac{\boldsymbol{\nabla} P}{\rho} + 2\mathbf{v} \times \boldsymbol{\Omega} + \nu\Delta\mathbf{v} + \mathbf{F}_{\rm st}, \qquad (1)$$

$$\frac{\partial \mathbf{W}}{\partial t} = \boldsymbol{\nabla} \times (\mathbf{v} \times \mathbf{W} + 2\mathbf{v} \times \boldsymbol{\Omega} - \nu \boldsymbol{\nabla} \times \mathbf{W}), \qquad (2)$$

where $\mathbf{v}$ is the fluid velocity with $\boldsymbol{\nabla}\cdot\mathbf{v}=0$, P is the fluid pressure, $\mathbf{F}_{\rm st}$ is an external stirring force with a zero mean value, $\boldsymbol{\Omega}$ is a constant angular velocity, and ν is the kinematic viscosity. Equation (2) follows from the Navier-Stokes equation (1). We use a mean-field approach whereby the velocity, pressure, and vorticity are separated into the mean and fluctuating parts, $\mathbf{v}=\overline{\mathbf{U}}+\mathbf{u}$, $P=\overline{P}+p$, and $\mathbf{W}=\overline{\mathbf{W}}+\mathbf{w}$, and the fluctuating parts have zero mean values, $\overline{\mathbf{U}}=\langle\mathbf{v}\rangle$, $\overline{P}=\langle P\rangle$, and $\overline{\mathbf{W}}=\langle\mathbf{W}\rangle$. Averaging Eqs. (1) and (2) over an ensemble of fluctuations we obtain the equations for the mean velocity $\overline{\mathbf{U}}$ and mean vorticity $\overline{\mathbf{W}}$:

$$\left[\frac{\partial}{\partial t} + \overline{\mathbf{U}} \cdot \boldsymbol{\nabla}\right]\overline{\mathbf{U}} = -\frac{\boldsymbol{\nabla} \overline{P}}{\rho} + 2\overline{\mathbf{U}} \times \boldsymbol{\Omega} + \boldsymbol{\mathcal{F}} + \nu\Delta\overline{\mathbf{U}}, \qquad (3)$$

$$\frac{\partial \overline{\mathbf{W}}}{\partial t} = \boldsymbol{\nabla} \times (\overline{\mathbf{U}} \times \overline{\mathbf{W}} + 2\overline{\mathbf{U}} \times \boldsymbol{\Omega} + \langle \mathbf{u} \times \mathbf{w}\rangle - \nu \boldsymbol{\nabla} \times \overline{\mathbf{W}}), \qquad (4)$$

where $\mathcal{F}_i = -\nabla_j \langle u_i u_j\rangle$. Note that the effect of turbulence on the mean vorticity is determined by the Reynolds stresses $\langle u_i u_j\rangle$ because

$$\langle \mathbf{u} \times \mathbf{w}\rangle_i = -\nabla_j\langle u_i u_j\rangle + \frac{1}{2}\nabla_i\langle \mathbf{u}^2\rangle. \qquad (5)$$

Consider a steady-state solution of Eqs. (3) and (4) in the form $\overline{\mathbf{U}}^{(s)}=\mathbf{0}$ and $\overline{\mathbf{W}}^{(s)}=\mathbf{0}$. In order to study a stability of this equilibrium we consider perturbations of the mean velocity $\tilde{\mathbf{U}}$ and the mean vorticity $\tilde{\mathbf{W}}$. The linearized equations for the small perturbations of the mean velocity and the mean vorticity are given by

$$\frac{\partial \tilde{\mathbf{U}}}{\partial t} = -\frac{\boldsymbol{\nabla}\tilde{P}}{\rho} + 2\tilde{\mathbf{U}} \times \boldsymbol{\Omega} + \tilde{\boldsymbol{\mathcal{F}}}(\tilde{\mathbf{U}}) + \nu\Delta\tilde{\mathbf{U}}, \qquad (6)$$

$$\frac{\partial \tilde{\mathbf{W}}}{\partial t} = \boldsymbol{\nabla} \times (2\tilde{\mathbf{U}} \times \boldsymbol{\Omega} + \tilde{\boldsymbol{\mathcal{F}}}(\tilde{\mathbf{U}}) - \nu \boldsymbol{\nabla} \times \tilde{\mathbf{W}}), \qquad (7)$$

where $\tilde{\boldsymbol{\mathcal{F}}}(\tilde{\mathbf{U}}) = -\nabla_j(f_{ij}-f_{ij}^{(0)})$ is the effective force, $f_{ij}=\langle u_i u_j\rangle$, and $f_{ij}^{(0)}$ is the second moment of the velocity field in a background turbulence (with a zero gradient of the mean velocity). Thus, the mean fields $\tilde{\mathbf{U}}$ and $\tilde{\mathbf{W}}$ represent deviations from the equilibrium solution $\overline{\mathbf{U}}^{(s)}=\mathbf{0}$ and $\overline{\mathbf{W}}^{(s)}=\mathbf{0}$. This equilibrium solution is a steady-state solution of Eqs. (3) and (4). Note that the characteristic times and spatial scales of small-scale fluctuations of velocity and vorticity $\mathbf{u}$ and $\mathbf{w}$ are much smaller than that of the mean fields $\tilde{\mathbf{U}}$ and $\tilde{\mathbf{W}}$.

In order to obtain a closed system of equations in the next section we derived an equation for the effective force $\tilde{\boldsymbol{\mathcal{F}}}$.

III. EFFECTIVE FORCE

In this section we derive an equation for the effective force $\tilde{\boldsymbol{\mathcal{F}}}$. The mean velocity gradients can affect turbulence. The reason is that additional essentially nonisotropic velocity fluctuations can be generated by tangling of the mean-velocity gradients with the Kolmogorov-type turbulence. The source of energy of this "tangling turbulence" is the energy of the Kolmogorov turbulence. The tangling turbulence was introduced by Wheelon [28] and Batchelor *et al.* [29] for a passive scalar and by Golitsyn [30] and Moffatt [31] for a passive vector (magnetic field). Anisotropic fluctuations of a passive scalar (e.g., the number density of particles or temperature) are generated by tangling of gradients of the mean passive scalar field with a random velocity field. Similarly, anisotropic magnetic fluctuations are excited by tangling of the mean magnetic field with the velocity fluctuations. The Reynolds stress in a turbulent flow with mean velocity gradients is another example of a tangling turbulence. Indeed, they are strongly anisotropic in the presence of mean velocity gradients and have a steeper spectrum ($\propto k^{-7/3}$) than a Kolmogorov turbulence (see, e.g., [32–36]). The anisotropic velocity fluctuations of tangling turbulence were studied first by Lumley [32].

To derive an equation for the effective force $\tilde{\boldsymbol{\mathcal{F}}}$ we use equation for fluctuations $\mathbf{u}(t,\mathbf{r})$ which is obtained by subtracting Eq. (3) for the mean field from Eq. (1) for the total field:

$$\frac{\partial \mathbf{u}}{\partial t} = -(\overline{\mathbf{U}} \cdot \boldsymbol{\nabla})\mathbf{u} - (\mathbf{u} \cdot \boldsymbol{\nabla})\overline{\mathbf{U}} - \frac{\boldsymbol{\nabla} p}{\rho} + 2\mathbf{u} \times \boldsymbol{\Omega} + \mathbf{F}_{\rm st} + \mathbf{U}^N, \qquad (8)$$

where

$$\mathbf{U}^N = \langle(\mathbf{u} \cdot \boldsymbol{\nabla})\mathbf{u}\rangle - (\mathbf{u} \cdot \boldsymbol{\nabla})\mathbf{u} + \nu\Delta\mathbf{u}. \qquad (9)$$

We consider a turbulent flow with large Reynolds numbers ($\mathrm{Re}=l_0 u_0/\nu \gg 1$), where u_0 is the characteristic velocity in the maximum scale l_0 of turbulent motions. We assume that there is a separation of scales; i.e., the maximum scale of turbulent motions l_0 is much smaller than the characteristic scale of inhomogeneities of the mean fields. Using Eq. (8)

we derived an equation for the second moment of the turbulent velocity field $f_{ij}(\mathbf{k},\mathbf{R}) \equiv \int \langle u_i(\mathbf{k}+\mathbf{K}/2) u_j(-\mathbf{k}+\mathbf{K}/2)\rangle \exp(i\mathbf{K}\cdot\mathbf{R}) d\mathbf{K}$:

$$\frac{\partial f_{ij}(\mathbf{k},\mathbf{R})}{\partial t} = \mathcal{G}_{ijmn} f_{mn} + F_{ij} + f_{ij}^{(N)} \tag{10}$$

(see Appendix A), where $\mathcal{G}_{ijmn}=I_{ijmn}(\tilde{\mathbf{U}})+N_{ijmn}(\mathbf{\Omega})$,

$$I_{ijmn}(\tilde{\mathbf{U}}) = \left[2k_{iq}\delta_{mp}\delta_{jn} + 2k_{jq}\delta_{im}\delta_{pn} - \delta_{im}\delta_{jq}\delta_{np} - \delta_{iq}\delta_{jn}\delta_{mp} + \delta_{im}\delta_{jn}k_q \frac{\partial}{\partial k_p}\right]\nabla_p \tilde{U}_q, \tag{11}$$

$$N_{ijmn}(\mathbf{\Omega}) = 2\Omega_q k_{pq}(\varepsilon_{imp}\delta_{nj} + \varepsilon_{jmp}\delta_{ni}), \tag{12}$$

and $\mathbf{R}$ and $\mathbf{K}$ correspond to the large scales, and $\mathbf{r}$ and $\mathbf{k}$ to the small scales (see Appendix A), δ_{ij} is the Kronecker tensor, $k_{ij}=k_ik_j/k^2$, and $\mathbf{\nabla}=\partial/\partial\mathbf{R}$, $F_{ij}(\mathbf{k},\mathbf{R})=\langle\tilde{F}_i(\mathbf{k},\mathbf{R})u_j\times(-\mathbf{k},\mathbf{R})\rangle+\langle u_i(\mathbf{k},\mathbf{R})\tilde{F}_j(-\mathbf{k},\mathbf{R})\rangle$, $\tilde{\mathbf{F}}(\mathbf{k},\mathbf{R},t)=-\mathbf{k}\times(\mathbf{k}\times\mathbf{F}_{\rm st}(\mathbf{k},\mathbf{R}))/k^2$, and $f_{ij}^{(N)}(\mathbf{k},\mathbf{R})$ are the terms which are related with the third moments appearing due to the nonlinear terms. The third moments terms $f_{ij}^{(N)}$ are defined as

$$f_{ij}^{(N)}(\mathbf{k},\mathbf{R}) = \langle P_{in}(\mathbf{k}_1)\hat{U}_n^N(\mathbf{k}_1)u_j(\mathbf{k}_2)\rangle + \langle u_i(\mathbf{k}_1)P_{jn}(\mathbf{k}_2)\hat{U}_n^N(\mathbf{k}_2)\rangle,$$

where $\hat{\mathbf{U}}_n^N(\mathbf{k})$ is the Fourier transform of $\mathbf{U}^N$ determined by Eq. (9), $\mathbf{k}_1=\mathbf{k}+\mathbf{K}/2$, $\mathbf{k}_2=-\mathbf{k}+\mathbf{K}/2$, and $P_{ij}(\mathbf{k})=\delta_{ij}-k_{ij}$.

Equation (10) is written in a frame moving with a local velocity $\tilde{\mathbf{U}}$ of the mean flow. In Eq. (10) for the second moments of the turbulent velocity field we neglected small terms $\sim O(\mathbf{\nabla}^2)$, where the terms with $\nabla \sim O(L^{-1})$ contain the large-scale spatial derivatives. These terms are of the order of $(l_0/L)^2$, where the maximum scale of turbulent motions l_0 is much smaller than the vertical size of the turbulent region L.

Equation (10) for the background turbulence (with a zero gradient of the mean fluid velocity $\nabla_i\tilde{\mathbf{U}}_j=0$ and $\mathbf{\Omega}=\mathbf{0}$) reads

$$\frac{\partial f_{ij}^{(0)}(\mathbf{k},\mathbf{R})}{\partial t} = F_{ij} + f_{ij}^{(N,0)}, \tag{13}$$

where the superscript (0) corresponds to the background turbulence, and we assumed that the tensor $F_{ij}(\mathbf{k},\mathbf{R})$, which is determined by a stirring force, is independent of the mean-velocity gradients and of a constant mean angular velocity. The equation for the deviations $f_{ij}-f_{ij}^{(0)}$ from the background turbulence is given by

$$\frac{\partial (f_{ij}-f_{ij}^{(0)})}{\partial t} = \mathcal{G}_{ijmn} f_{mn} + f_{ij}^{(N)} - f_{ij}^{(N,0)}. \tag{14}$$

Equation (14) for the deviations of the second moments $f_{ij}-f_{ij}^{(0)}$ in $\mathbf{k}$ space contains the deviations of the third moments $f_{ij}^{(N)}-f_{ij}^{(N,0)}$ and a problem of closing the equations for the higher moments arises. Various approximate methods have been proposed for the solution of problems of this type (see, e.g., [37–39]). The simplest procedure is the τ approximation which was widely used for study of different problems of turbulent transport (see, e.g., [37,40–43]). One of the simplest procedures, which allows us to express the deviations of the terms with the third moments $f_{ij}^{(N)}-f_{ij}^{(N,0)}$ in $\mathbf{k}$ space in terms of that for the second moments $f_{ij}-f_{ij}^{(0)}$, reads

$$f_{ij}^{(N)} - f_{ij}^{(N,0)} = -\frac{f_{ij}-f_{ij}^{(0)}}{\tau(k)}, \tag{15}$$

where $\tau(k)$ is the scale-dependent correlation time of the turbulent velocity field. Here we assumed that the time $\tau(k)$ is independent of the mean velocity gradients (for a weak mean-velocity shear). We considered also the case of a slow rotation rate. In this case a modification of the correlation time of fully developed turbulence by slow rotation is small. This allows us to suggest that Eq. (15) is valid for a slow rotation rate.

The τ approximation is different from eddy-damped quasinormal Markovian (EDQNM) approximation. A principal difference between these two approaches is as follows (see [37,39]). The EDQNM closures do not relax to the equilibrium, and this procedure does not describe properly the motions in the equilibrium state. In the EDQNM approximation, there is no dynamically determined relaxation time, and no slightly perturbed steady state can be approached [37]. In the τ approximation, the relaxation time for small departures from equilibrium is determined by the random motions in the equilibrium state, but not by the departure from equilibrium [37]. The analysis performed in [37] showed that the τ approximation describes the relaxation to the equilibrium state (the background turbulence) more accurately than the EDQNM approach.

Note that we applied the τ approximation (15) only to study the deviations from the background turbulence which are caused by the spatial derivatives of the mean velocity and a uniform rotation. The background turbulence is assumed to be known. Here we use the following model for the background isotropic and weakly inhomogeneous turbulence:

$$f_{ij}^{(0)}(\mathbf{k},\mathbf{R}) = \frac{\mathcal{E}(k)}{8\pi k^2}\left[P_{ij}(\mathbf{k}) + \frac{i}{2k^2}(k_i\nabla_j - k_j\nabla_i)\right]\langle\mathbf{u}^2\rangle^{(0)} \tag{16}$$

(see, e.g., [44]), where $P_{ij}(\mathbf{k})=\delta_{ij}-k_{ij}$, δ_{ij} is the Kronecker tensor, and $k_{ij}=k_ik_j/k^2$, $\tau(k)=2\tau_0\bar{\tau}(k)$, $\mathcal{E}(k)=-d\bar{\tau}(k)/dk$, $\bar{\tau}(k)=(k/k_0)^{1-q}$, $1<q<3$ is the exponent of the kinetic energy spectrum (e.g., $q=5/3$ for Kolmogorov spectrum), and $k_0=1/l_0$.

The mean-velocity gradient $\nabla_i\tilde{\mathbf{U}}$ causes generation of anisotropic velocity fluctuations (tangling turbulence). Equations (14)–(16) allow us to determine the second moment $f_{ij}(\mathbf{R})=\int f_{ij}(\mathbf{k},\mathbf{R})d\mathbf{k}$:

$$f_{ij}(\mathbf{R}) = f_{ij}^{(0)}(\mathbf{R}) - \nu_T^{(0)}M_{ij} - \frac{1}{6}l_0^2\Omega S_{ij} \tag{17}$$

(see Appendix B), where $\nu_T^{(0)}=\tau_0\langle\mathbf{u}^2\rangle^{(0)}/6$ and the tensors M_{ij} and S_{ij} are determined in Appendix B. The definition of the function $\nu_T^{(0)}$ yields $\langle\mathbf{u}^2\rangle^{(0)}(\mathbf{R})=6\nu_T^{(0)}(\mathbf{R})/\tau_0$. Since we assumed that τ_0 is independent of $\mathbf{R}$, the spatial profile of the function $\nu_T^{(0)}$ [e.g., given by Eq. (26) in Sec. IV B] determines the spatial profile of $\langle \mathbf{u}^2 \rangle^{(0)}$. Equation (17) allows us to determine the effective force $\tilde{\mathcal{F}}_i = -\nabla_j [f_{ij}(\mathbf{R}) - f_{ij}^{(0)}(\mathbf{R})]$:

$$\tilde{\mathcal{F}}_i = \nu_T^{(0)}(M_{ij}\Lambda_j + \nabla_j M_{ij}) + \frac{1}{6} l_0^2 \Omega (S_{ij}\Lambda_j + \nabla_j S_{ij}), \qquad (18)$$

where $\mathbf{\Lambda} = (\mathbf{\nabla} l_0^2)/l_0^2 = (\mathbf{\nabla} \nu_T^{(0)})/\nu_T^{(0)}$.

Note that when Λ=const and the velocity field is incompressible, the effective force $\tilde{\boldsymbol{\mathcal{F}}}$ does not have the term $\propto \alpha \tilde{\mathbf{W}}$, where α describes the hydrodynamic α effect. The hydrodynamic α effect was introduced in the equation for the mean vorticity (see, e.g., [4,6,7]), similarly to the α effect in the equation for the evolution of the mean magnetic field (see, e.g., [45]). The reason for the absence of the $\alpha \tilde{\mathbf{W}}$ term in $\tilde{\boldsymbol{\mathcal{F}}}$ is as follows. Let us suggest the opposite—i.e., that $\tilde{\boldsymbol{\mathcal{F}}} \propto \alpha \tilde{\mathbf{W}} = \alpha \mathbf{\nabla} \times \tilde{\mathbf{U}}$. Since the effective force $\tilde{\mathcal{F}}_i = -\nabla_j [f_{ij}(\mathbf{R}) - f_{ij}^{(0)}(\mathbf{R})]$, we obtain

$$f_{ij}(\mathbf{R}) - f_{ij}^{(0)}(\mathbf{R}) \propto -\alpha \varepsilon_{ijk} \tilde{U}_k. \qquad (19)$$

Here we used the identity $\tilde{W}_i = \varepsilon_{ijk} \nabla_j \tilde{U}_k$ and we took into account that when Λ=const, the hydrodynamic α is constant. Note also that in our paper we considered incompressible velocity field. The condition (19) is in contradiction with the Galilean invariance, because the Reynolds stresses in the considered case may depend on the gradient of the mean-velocity field rather than on the mean velocity itself. When Λ is not constant, the effective force $\tilde{\boldsymbol{\mathcal{F}}}$ can have the term $\propto \alpha \tilde{\mathbf{W}}$. However, this effect is not in the scope of our paper (e.g., this case cannot be described in the framework of the gradient approximation).

IV. LARGE-SCALE INSTABILITY IN AN INHOMOGENEOUS TURBULENCE

For simplicity we consider the case when the turbulence is inhomogeneous along the rotation axis—i.e., $\mathbf{\Lambda} = \Lambda \mathbf{e}_z$, $\mathbf{\Omega} = \Omega \mathbf{e}_z$. After calculating $[\mathbf{\nabla} \times (\mathbf{\nabla} \times \tilde{\mathbf{U}})]_z$ from Eq. (6) and $\tilde{W}_z$ from Eq. (7) we arrive at the following equations written in nondimensional form:

$$\Delta \frac{\partial \tilde{U}_z}{\partial t} = -[\hat{G} - \beta_U \Delta_\perp \nabla_z] \tilde{W}_z + [\nu_T \Delta^2 + \nu_T \Lambda \Delta \nabla_z + \nu_U \Lambda \Delta_\perp \nabla_z + \eta_U \Delta_\perp \nabla_z^2] \tilde{U}_z, \qquad (20)$$

$$\frac{\partial \tilde{W}_z}{\partial t} = (\hat{G} - \beta \Lambda \Delta_\perp) \tilde{U}_z + [\nu_T \nabla_z^2 + \nu_T \Lambda \nabla_z + \eta_W \Delta_\perp] \tilde{W}_z, \qquad (21)$$

where $\Delta = \Delta_\perp + \nabla_z^2$, $\nabla_z = \partial / \partial z$,

$$\hat{G} = 2 a_* \nabla_z + \beta [\Lambda \nabla_z^2 + \Delta \nabla_z],$$

$$\beta(\Omega, z) = \nu_T^{(0)}(z)(\omega/8)[D_5(\omega)/2 - D_6(\omega)],$$

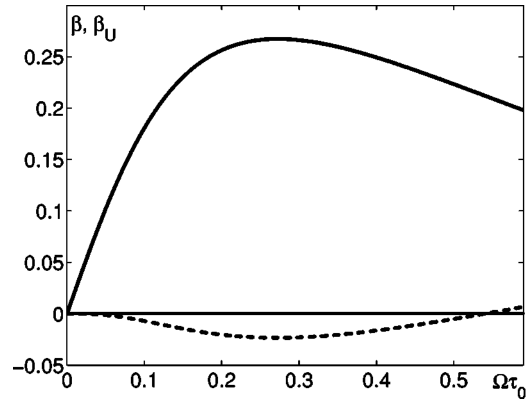

FIG. 1. The rotation rate dependence of the functions $\beta(\Omega\tau_0)$ (solid line) and $\beta_U(\Omega\tau_0)$ (dashed line).

$$\beta_U(\Omega, z) = \nu_T^{(0)}(z)(\omega/8) D_6(\omega),$$

$$\nu_T(\Omega, z) = \nu_T^{(0)}(z)[D_1(\omega)/2 + D_2(\omega)],$$

$$\nu_U(\Omega, z) = \eta_U(\Omega, z) + 2\nu_T^{(0)}(z) D_2(\omega),$$

$$\eta_U(\Omega, z) = \nu_T^{(0)}(z) D_4(\omega),$$

$$\eta_W(\Omega, z) = \nu_T^{(0)}(z)[D_1(\omega)/2 - D_3(\omega)].$$

Here $\omega = 8\tau_0 \Omega$, $a_* = \Omega L^2/\nu_T^* \gg 1$, and we used Eq. (18). The functions $D_k(\omega)$ are determined in Appendix B.

In Eqs. (20) and (21) we use the following dimensionless variables: length is measured in units of L, time in units of L^2/ν_T^*, the parameter Λ is measured in the units of L^{-1}, the function $\nu_T^{(0)}(z)$ is measured in the units of ν_T^*, and the perturbations of velocity $\tilde{U}_z$ and vorticity $\tilde{W}_z$ are measured in units of U_* and U_*/L, respectively. The functions $\beta(\Omega\tau_0)$, $\beta_U(\Omega\tau_0)$, $\nu_T(\Omega\tau_0)$, $\nu_U(\Omega\tau_0)$, $\eta_W(\Omega\tau_0)$, and $\eta_U(\Omega\tau_0)$ are shown in Figs. 1 and 2. All these functions shown in Figs. 1 and 2 are normalized by $\nu_T^{(0)}(z)$—e.g., $\nu_T(\Omega\tau_0) \equiv \nu_T(\Omega, z)/\nu_T^{(0)}(z)$—and similarly for other functions.

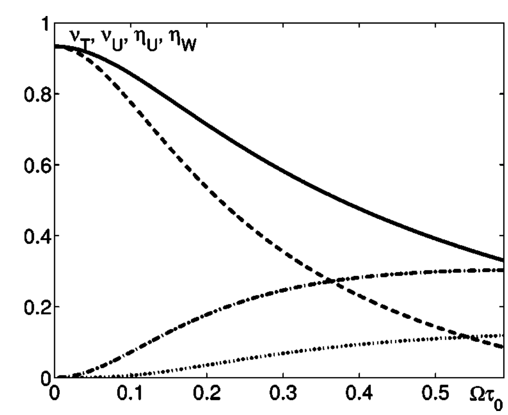

FIG. 2. The rotation rate dependence of the functions $\nu_T(\Omega\tau_0)$ (solid line), $\nu_U(\Omega\tau_0)$ (dash-dotted line), $\eta_W(\Omega\tau_0)$ (dashed line), and $\eta_U(\Omega\tau_0)$ (dotted line).

A. Weakly inhomogeneous turbulence

Assume that functions $\nu_T^{(0)}(z)$ and $\Lambda(z)$ vary slowly with z in comparison with the variations of the mean velocity $\tilde{U}_z(z)$ and mean vorticity $\tilde{W}_z(z)$. Let us seek a solution of Eqs. (20) and (21) in the form $\propto \exp(\gamma t - i\mathbf{K}\cdot\mathbf{R})$. Let us first consider perturbations with the wave numbers $K_\perp^2 \ll K_z^2$. Since $\boldsymbol{\nabla}\cdot\tilde{\mathbf{U}}=0$, the velocity components $\tilde{U}_z \ll |\tilde{\mathbf{U}}_\perp|$. Thus the growth rate of the inertial waves with frequency

$$\omega_w = -\,\mathrm{sgn}(\beta\Lambda)\frac{2a_* K_z}{K} \tag{22}$$

is given by

$$\gamma_w = |\beta(\Omega\tau_0)\Lambda K_z| - \nu_T(\Omega\tau_0)K^2, \tag{23}$$

where $\gamma=\gamma_w+i\omega_w$, the wave number K is measured in the units of L^{-1}, and γ is measured in the units of ν_T^*/L^2. The maximum growth rate of the inertial waves, $\gamma_m=[\beta(\Omega\tau_0)\Lambda]^2/4\nu_T(\Omega\tau_0)$, is attained at $K=K_m=|\beta(\Omega\tau_0)\Lambda|/2\nu_T(\Omega\tau_0)$. For a very small rotation rate—i.e., for $\omega\equiv 8\Omega\tau_0 \ll 1$—the turbulent viscosity $\nu_T(\Omega\tau_0)\approx(q+3)/5$ and $\beta(\Omega\tau_0)\approx(32/15)\Omega\tau_0$, where the parameter q is the exponent of the kinetic energy spectrum of the background isotropic and weakly inhomogeneous turbulence (e.g., $q=5/3$ for Kolmogorov spectrum), and this parameter varies in the range $1<q<3$. Note that the inertial waves are helical; i.e., the large-scale hydrodynamic helicity of the motions in the inertial waves is $\tilde{\mathbf{U}}\cdot(\boldsymbol{\nabla}\times\tilde{\mathbf{U}})=2|\tilde{\mathbf{U}}_\perp|^2K_z\neq 0$. This instability is caused by a combined effect of the inhomogeneity of the turbulence and the uniform mean rotation [see the first term in Eq. (23)].

Now we consider the opposite case—i.e., the perturbations with the wave numbers $K_\perp^2 \gg K_z^2$. Since $\boldsymbol{\nabla}\cdot\tilde{\mathbf{U}}=0$, the velocity components $\tilde{U}_z \gg |\tilde{\mathbf{U}}_\perp|$. When $K^2|\beta(\Omega)\Lambda|/4a_* \ll K_z \ll K_\perp$, the growth rate of perturbations with frequency

$$\omega_w = \mathrm{sgn}(\beta\Lambda)\frac{2a_* K_z}{K}, \tag{24}$$

is given by

$$\gamma_w = \frac{1}{2}[|\beta(\Omega\tau_0)\Lambda|K - [\nu_T(\Omega\tau_0)+\eta_W(\Omega\tau_0)]K^2]. \tag{25}$$

The maximum growth rate of perturbations, $\gamma_m=[\beta(\Omega\tau_0)\Lambda]^2/8[\nu_T(\Omega\tau_0)+\eta_W(\Omega\tau_0)]$, is attained at $K=K_m=|\beta(\Omega\tau_0)\Lambda|/2[\nu_T(\Omega\tau_0)+\eta_W(\Omega\tau_0)]$. This case corresponds to $a_* \gg \beta^2(\Omega\tau_0)/4\nu_T(\Omega\tau_0)$. The large-scale hydrodynamic helicity of the flow is $\tilde{\mathbf{U}}\cdot(\boldsymbol{\nabla}\times\tilde{\mathbf{U}})=4K_\perp|\tilde{\mathbf{U}}_z|^2\,\mathrm{sgn}(\beta)\neq 0$.

B. Numerical results

In this section we take into account the inhomogeneity of the functions $\nu_T^{(0)}(z)$ and $\Lambda(z)$. Consider an eigenvalue problem for a system of Eqs. (20) and (21). We seek for a solution of Eqs. (20) and (21) in the form $\propto\Psi(z)\exp(\gamma t)J_0(K_\perp r)$, where $J_0(x)$ is the Bessel function of the first kind. After substitution of this solution into Eqs. (20) and (21) we obtain the system of ordinary differential equations which is solved numerically.

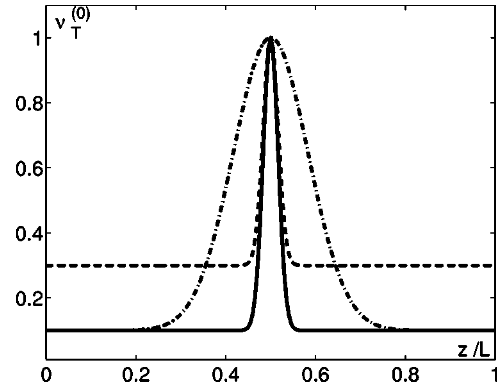

FIG. 3. The vertical profile of the turbulent viscosity $\nu_T^{(0)}(z)$ for $\Lambda_0=30$ and $\nu_T^{(b)}=0.1$ (solid line), $\Lambda_0=30$ and $\nu_T^{(b)}=0.3$ (dashed line), $\Lambda_0=12$ and $\nu_T^{(b)}=0.1$ (dash-dotted line).

We used the cylindrical geometry (z,r,ϕ) with the z axis along the rotation axis and consider the axisymmetric solution (i.e., there are no derivatives with respect to the polar angle ϕ). The turbulence is inhomogeneous along the rotation axis. We use the periodic boundary conditions in the z direction for Eqs. (20) and (21)—i.e., $\tilde{U}_z(z=0,r)=\tilde{U}_z(z=L,r)$, $\tilde{U}_z'(z=0,r)=\tilde{U}_z'(z=L,r)$, $\tilde{U}_z''(z=0,r)=\tilde{U}_z''(z=L,r)$, $\tilde{U}_z'''(z=0,r)=\tilde{U}_z'''(z=L,r)$, $\tilde{W}_z(z=0,r)=\tilde{W}_z(z=L,r)$, and $\tilde{W}_z'(z=0,r)=\tilde{W}_z'(z=L,r)$, where $\tilde{f}'=\nabla_z\tilde{f}$. We also use the condition $\tilde{U}_r(z,r=0)=\tilde{U}_r(z,r=R)=0$, where R is the radius of the turbulent region.

We have chosen the vertical spatial profile of the function $\nu_T^{(0)}(z)$ in the form

$$\nu_T^{(0)}(z) = 1 - C\left\{1-\exp\left[-2\Lambda_0^2\left(\frac{z}{L}-\frac{1}{2}\right)^2\right]\right\},$$

$$C = \frac{1-\nu_T^{(b)}}{1-\exp(-\Lambda_0^2/2)}, \tag{26}$$

with two values of the parameter $\nu_T^{(b)}=0.1$ and 0.3 and two values of the parameter $\Lambda_0=12$ and 30. The vertical profile of the turbulent viscosity $\nu_T^{(0)}(z)$ is shown in Fig. 3. The maximum of turbulence intensity is located at $z=L/2$. The form of the chosen spatial profile of the function $\nu_T^{(0)}(z)$ is simple enough and universal. It allows us to vary the size of the region occupied by turbulence (by changing the parameter Λ_0) and the difference in the level of the turbulence between the center and boundary of the region (by changing the parameter $\nu_T^{(b)}$); i.e., it allows us to change the inhomogeneity of the turbulence. The numerical solution of Eqs. (20) and (21) was performed also for other spatial profiles of the function $\nu_T^{(0)}(z)$. However, the final results do not depend strongly on the details in the spatial profile of the function $\nu_T^{(0)}(z)$. Note also that the chosen spatial profile of the function $\nu_T^{(0)}(z)$ can mimic the distribution of turbulence in galactic and accretion discs (see, e.g., [46]).

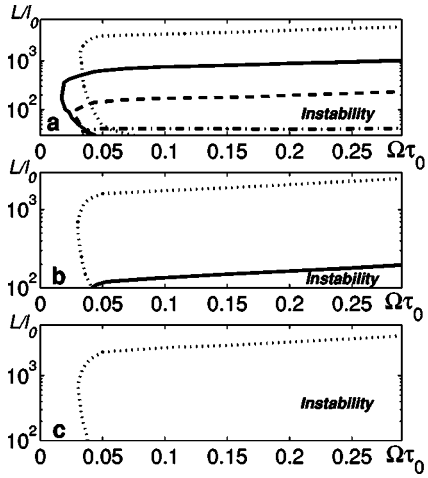

FIG. 4. The range of parameters $(L/l_0, \Omega\tau_0)$ for which the large-scale instability occurs $(\gamma_w > 0)$ for (a) $\Lambda_0=12$, $\nu_T^{(b)}=0.1$; (b) $\Lambda_0=30$, $\nu_T^{(b)}=0.1$; (c) $\Lambda_0=30$, $\nu_T^{(b)}=0.3$; and different values of the parameter μ: $\mu=0.1$ (dotted line), $\mu=0.5$ (solid line), $\mu=1$ (dashed line), $\mu=2$ (dash-dotted line).

The sufficient condition for the excitation of the instability is $\gamma_w > 0$. The range of parameters $(L/l_0, \Omega\tau_0)$ for which the large-scale instability occurs is shown in Fig. 4 for different values of the parameters μ, $\nu_T^{(b)}(z)$, and Λ_0. Here $\mu=L/L_r$, L is the vertical size of the whole region, and L_r is a radius from the center of the structure at which the energy $\tilde{U}_r^2$ of the radial velocity perturbations is maximum. Note that the maximum radial (horizontal) size R of the whole region is of the order of $\sim 4L_r$. The decrease of the parameter μ causes increase of the range of the large-scale instability. On the other hand, the increase of the size of the highly intense turbulent region (i.e., decrease of the parameter Λ_0) results in the increase of the range of the instability.

The rotation rate dependences of the growth rate $\gamma_w\tau_D$ of the large-scale instability and the frequency $\omega_w\tau_0$ of the generated waves due to the large-scale instability are shown in Figs. 5 and 6, where $\tau_D=L^2/\nu_T^*$. There is a threshold in the rotation rate for the large-scale instability, $\Omega_*\tau_0 \approx 0.025$, and when $\Omega > \Omega_*$, the instability is excited. The instability threshold in the parameter L is $L > 10 l_0$.

Note that the characteristic time $(\sim 2\pi/\gamma_w)$ of the growth of perturbations of the mean fields $\tilde{\mathbf{U}}$ and $\tilde{\mathbf{W}}$ is by five orders of magnitudes larger than the turbulent correlation time τ_0. The period of oscillations, $T=2\pi/\omega_w$, of inertial waves is at least 10 times larger than the turbulent correlation time τ_0. The minimum value of the period of rotation $T_R=2\pi/\Omega$ is at least 20 times larger than the turbulent correlation time τ_0. All spatial scales: the vertical size of the turbulent region, L, and the vertical size of the highly intense turbulence $(\sim L/\Lambda_0)$ are much larger than the maximum scale of turbulent motions l_0 (e.g., L/Λ_0 is at least 10 times larger than the maximum scale of turbulent motions l_0). This implies that there is indeed a separation of scales as we assumed in the derivations. Note also that the range of validity of the obtained results is $\tau_0 \ll T$ for a statistically stationary background turbulence. In particular, we assumed that the characteristic time of evolution of the second moments is much smaller than the turbulent correlation time. The asymptotic formulas (22)–(25) are in agreement with the obtained numerical results.

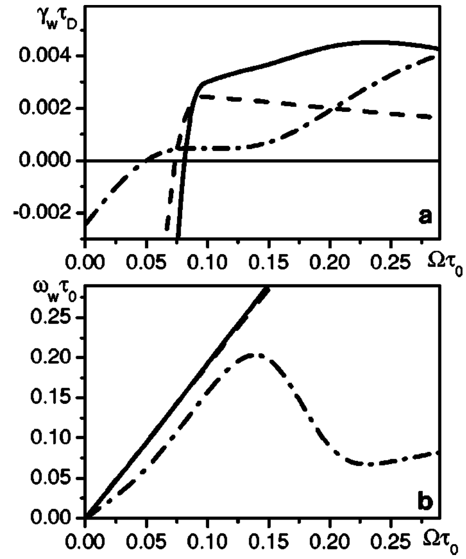

FIG. 5. The rotation rate $(\Omega\tau_0)$ dependences of (a) the growth rate $\gamma_w\tau_D$ of the large-scale instability and (b) the frequency $\omega_w\tau_0$ of the generated waves due to the large-scale instability for $\Lambda_0=12$, $\nu_T^{(b)}=0.1$, $\mu=0.1$, and different values of the parameter L/l_0: $L/l_0=50$ (solid line), $L/l_0=100$ (dashed line), and $L/l_0=500$ (dash-dotted line). Here $\tau_D=L^2/\nu_T^*$.

It must be noted that turbulent flow with an imposed mean linear velocity shear and uniformly rotating flows are essentially different. In particular, in a turbulent flow with an imposed mean linear velocity shear there are no waves similar to the inertial waves which exist in a uniformly rotating flows. The reason is that any shear motions have a nonzero

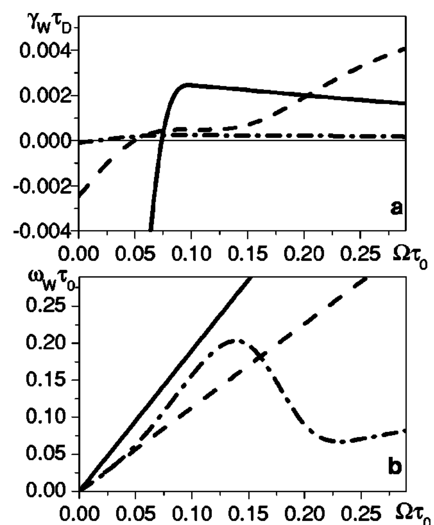

FIG. 6. The rotation rate $(\Omega\tau_0)$ dependences of (a) the growth rate $\gamma_w\tau_D$ of the large-scale instability and (b) the frequency $\omega_w\tau_0$ of the generated waves due to the large-scale instability for $\Lambda_0=30$, $\nu_T^{(b)}=0.1$, $\mu=0.1$, and different values of the parameter L/l_0: $L/l_0=100$ (solid line), $L/l_0=500$ (dashed line), and $L/l_0=1000$ (dash-dotted line).

symmetric part $(\partial\hat{U})_{ij}$ of the gradient of the mean velocity, where $(\partial\hat{U})_{ij}=(\nabla_i\overline{U}_j+\nabla_j\overline{U}_i)/2$. In addition, the difference between these two flows is that the mean velocity shear produces work in a turbulent flow, while a uniform rotation does not produce work in homogeneous turbulent flow.

V. CONCLUSIONS

We studied formation of large-scale structures in a rotating inhomogeneous nonhelical turbulence. We found a mechanism for the excitation of the large-scale inertial waves which is associated with a generation of a large-scale vorticity due to the excitation of the large-scale instability in a uniformly rotating inhomogeneous turbulence. It was shown that the mean vorticity cannot be generated by a homogeneous uniformly rotating nonhelical turbulence. The excitation of the mean vorticity in this flow requires also an inhomogeneity of turbulence. Therefore, the large-scale instability is caused by a combined effect of the inhomogeneity of the turbulence and the uniform mean rotation. The source of the large-scale instability is the energy of the small-scale turbulence. The rotation and inhomogeneity of turbulence provide a mechanism for transport of energy from turbulence to large-scale motions. We determined the range of parameters at which the large-scale instability occurs.

Some of the results obtained in this study—e.g., the expression for the effective force in a homogeneous turbulence—are in compliance with the previous studies of rotating turbulence [49] [see Appendix B, Eq. (B13)]. It is plausible to suggest that the results of recent experiments [50] can be explained by the large-scale instability discussed in this paper. Direct quantitative comparison of our theoretical predictions with the experimental results reported in [50] is not feasible. The reason is that turbulent flow in the experimental setup used in [50] is inhomogeneous in radial and axial directions, and the radial inhomogeneity is stronger than the axial one. In our study we investigated the large-scale instability in the case of the axial inhomogeneity of turbulence and considered only a simple physical mechanisms to describe the initial stage of mean-vorticity generation in a rotating inhomogeneous turbulence. However, the main mechanism of the generation of the secondary flow in the experiments [50] is associated with the Reynolds stress-induced generation of the mean vorticity by a rotating inhomogeneous turbulence that was analyzed in our study. Clearly, the simple model considered in our investigation can only mimic the flow observed in the experiments [50], and comprehensive theoretical and numerical studies are required for their quantitative description.

ACKNOWLEDGMENTS

This work was partially supported by The German-Israeli Project Cooperation (DIP) administered by the Federal Ministry of Education and Research (BMBF) and by the Israel Science Foundation governed by the Israeli Academy of Science.

APPENDIX A: DERIVATION OF Eq. (10)

In order to derive Eq. (10) we use a mean-field approach; i.e., a correlation function is written as follows:

$$\langle u_i(\mathbf{x})u_j(\mathbf{y})\rangle = \int \langle u_i(\mathbf{k}_1)u_j(\mathbf{k}_2)\rangle \exp[i(\mathbf{k}_1\cdot\mathbf{x}+\mathbf{k}_2\cdot\mathbf{y})]d\mathbf{k}_1 d\mathbf{k}_2 = \int f_{ij}(\mathbf{k},\mathbf{R})\exp(i\mathbf{k}\cdot\mathbf{r})d\mathbf{k},$$

$$f_{ij}(\mathbf{k},\mathbf{R}) = \int \langle u_i(\mathbf{k}+\mathbf{K}/2)u_j(-\mathbf{k}+\mathbf{K}/2)\rangle \exp(i\mathbf{K}\cdot\mathbf{R})d\mathbf{K}$$

(see, e.g., [47,48]), where $\mathbf{R}$ and $\mathbf{K}$ correspond to the large scales and $\mathbf{r}$ and $\mathbf{k}$ to the small scales—i.e., $\mathbf{R}=(\mathbf{x}+\mathbf{y})/2$, $\mathbf{r}=\mathbf{x}-\mathbf{y}$, $\mathbf{K}=\mathbf{k}_1+\mathbf{k}_2$, and $\mathbf{k}=(\mathbf{k}_1-\mathbf{k}_2)/2$. This implies that we assumed that there exists a separation of scales; i.e., the maximum scale of turbulent motions l_0 is much smaller then the characteristic scale of inhomogeneities of the mean fields.

Now we calculate

$$\frac{\partial f_{ij}(\mathbf{k}_1,\mathbf{k}_2)}{\partial t} \equiv \left\langle P_{in}(\mathbf{k}_1)\frac{\partial u_n(\mathbf{k}_1)}{\partial t}u_j(\mathbf{k}_2)\right\rangle + \left\langle u_i(\mathbf{k}_1)P_{jn}(\mathbf{k}_2)\frac{\partial u_n(\mathbf{k}_2)}{\partial t}\right\rangle, \tag{A1}$$

where we multiplied equation of motion (8) rewritten in $\mathbf{k}$ space by $P_{ij}(\mathbf{k})=\delta_{ij}-k_{ij}$ in order to exclude the pressure term from the equation of motion, δ_{ij} is the Kronecker tensor, and $k_{ij}=k_ik_j/k^2$. This yields the equation for $f_{ij}(\mathbf{k},\mathbf{R})$ [see Eq. (10)]. For the derivation of Eq. (10) we used the equation

$$ik_i\int f_{ij}\left(\mathbf{k}-\frac{1}{2}\mathbf{Q},\mathbf{K}-\mathbf{Q}\right)\tilde{U}_p(\mathbf{Q})\exp(i\mathbf{K}\cdot\mathbf{R})d\mathbf{K}d\mathbf{Q} = -\frac{1}{2}\tilde{U}_p\nabla_i f_{ij}+\frac{1}{2}f_{ij}\nabla_i\tilde{U}_p-\frac{i}{4}(\nabla_s\tilde{U}_p)\left(\nabla_i\frac{\partial f_{ij}}{\partial k_s}\right) + \frac{i}{4}\left(\frac{\partial f_{ij}}{\partial k_s}\right)(\nabla_s\nabla_i\tilde{U}_p). \tag{A2}$$

To derive Eq. (A2) we multiply the equation $\boldsymbol{\nabla}\cdot\mathbf{u}=0$, written in $\mathbf{k}$ space for $u_i(\mathbf{k}_1-\mathbf{Q})$, by $u_j(\mathbf{k}_2)\tilde{U}_p(\mathbf{Q})\exp(i\mathbf{K}\cdot\mathbf{R})$, and integrate over $\mathbf{K}$ and $\mathbf{Q}$ and average over the ensemble of velocity fluctuations. Here $\mathbf{k}_1=\mathbf{k}+\mathbf{K}/2$ and $\mathbf{k}_2=-\mathbf{k}+\mathbf{K}/2$. This yields

$$\int i\left(k_i+\frac{1}{2}K_i-Q_i\right)\left\langle u_i\left(\mathbf{k}+\frac{1}{2}\mathbf{K}-\mathbf{Q}\right)u_j\left(-\mathbf{k}+\frac{1}{2}\mathbf{K}\right)\right\rangle \times\tilde{U}_p(\mathbf{Q})\exp(i\mathbf{K}\cdot\mathbf{R})d\mathbf{K}d\mathbf{Q}=0. \tag{A3}$$

Next, we introduce new variables: $\tilde{\mathbf{k}}_1=\mathbf{k}+\mathbf{K}/2-\mathbf{Q}$, $\tilde{\mathbf{k}}_2=-\mathbf{k}+\mathbf{K}/2$, $\tilde{\mathbf{k}}=(\tilde{\mathbf{k}}_1-\tilde{\mathbf{k}}_2)/2=\mathbf{k}-\mathbf{Q}/2$, and $\tilde{\mathbf{K}}=\tilde{\mathbf{k}}_1+\tilde{\mathbf{k}}_2=\mathbf{K}-\mathbf{Q}$. This allows us to rewrite Eq. (A3) in the form

$$\int i\left(k_i + \frac{1}{2}K_i - Q_i\right) f_{ij}\left(\mathbf{k} - \frac{1}{2}\mathbf{Q}, \mathbf{K} - \mathbf{Q}\right) \tilde{U}_p(\mathbf{Q}) \times \exp(i\mathbf{K}\cdot\mathbf{R}) d\mathbf{K} d\mathbf{Q} = 0. \quad (A4)$$

Since $|\mathbf{Q}| \ll |\mathbf{k}|$, we can use the Taylor series expansion

$$f_{ij}(\mathbf{k} - \mathbf{Q}/2, \mathbf{K} - \mathbf{Q}) \simeq f_{ij}(\mathbf{k}, \mathbf{K} - \mathbf{Q}) - \frac{1}{2}\frac{\partial f_{ij}(\mathbf{k}, \mathbf{K} - \mathbf{Q})}{\partial k_s} Q_s + O(\mathbf{Q}^2). \quad (A5)$$

We also use the following identities:

$$[f_{ij}(\mathbf{k}, \mathbf{R}) \tilde{U}_p(\mathbf{R})]_{\mathbf{K}} = \int f_{ij}(\mathbf{k}, \mathbf{K} - \mathbf{Q}) \tilde{U}_p(\mathbf{Q}) d\mathbf{Q},$$

$$\nabla_p [f_{ij}(\mathbf{k}, \mathbf{R}) \tilde{U}_p(\mathbf{R})] = \int iK_p [f_{ij}(\mathbf{k}, \mathbf{R}) \tilde{U}_p(\mathbf{R})]_{\mathbf{K}} \times \exp(i\mathbf{K}\cdot\mathbf{R}) d\mathbf{K}, \quad (A6)$$

where $[f_{ij}(\mathbf{k}, \mathbf{R}) \tilde{U}_p(\mathbf{R})]_{\mathbf{K}}$ denotes a Fourier transformation. Therefore, Eqs. (A4)–(A6) yield Eq. (A2).

APPENDIX B: THE REYNOLDS STRESSES

In this appendix we derive equation for the Reynolds stresses using Eq. (14). We assume that the characteristic time of variation of the second moment $f_{ij}(\mathbf{k}, \mathbf{R})$ is substantially larger than the correlation time $\tau(k)$ for all turbulence scales. Thus in a steady state Eq. (14) reads

$$[\hat{L}(\mathbf{\Omega}) - \tau(k)\hat{I}(\tilde{\mathbf{U}})](\hat{f} - \hat{f}^{(0)}) = \tau(k)[\hat{N}(\mathbf{\Omega}) + \hat{I}(\tilde{\mathbf{U}})]\hat{f}^{(0)}, \quad (B1)$$

where we used Eq. (15). Hereafter we use the following notation: $\hat{f} \equiv f_{ij}(\mathbf{k}, \mathbf{R})$, $\hat{f}^{(N)} \equiv f_{ij}^{(N)}(\mathbf{k}, \mathbf{R})$, $\hat{f}^{(0)} \equiv f_{ij}^{(0)}(\mathbf{k}, \mathbf{R})$, $\hat{I}(\tilde{\mathbf{U}})\hat{f} \equiv I_{ijmn}(\tilde{\mathbf{U}}) f_{mn}(\mathbf{k}, \mathbf{R})$ and $\hat{N}(\mathbf{\Omega})\hat{f} \equiv N_{ijmn}(\mathbf{\Omega}) f_{mn}(\mathbf{k}, \mathbf{R})$, and $\hat{L}(\mathbf{\Omega}) \equiv L_{ijmn}(\mathbf{\Omega}) = \delta_{im}\delta_{jn} - \tau(k) N_{ijmn}(\mathbf{\Omega})$. Multiplying Eq. (B1) by the inverse operator $\hat{L}^{-1}(\mathbf{\Omega})$ yields

$$[\hat{E} - \tau(k)\hat{L}^{-1}(\mathbf{\Omega})\hat{I}(\tilde{\mathbf{U}})](\hat{f} - \hat{f}^{(0)}) = -[\hat{E} - \hat{L}^{-1}(\mathbf{\Omega}) - \tau(k)\hat{L}^{-1}(\mathbf{\Omega})\hat{I}(\tilde{\mathbf{U}})]\hat{f}^{(0)}, \quad (B2)$$

where $\hat{E} \equiv \delta_{im}\delta_{jn}$, and we used an identity

$$\hat{E} - \hat{L}^{-1}(\mathbf{\Omega}) = -\tau(k)\hat{L}^{-1}(\mathbf{\Omega})\hat{N}(\mathbf{\Omega}).$$

The latter identity follows from the definition $\hat{L}^{-1}(\mathbf{\Omega})\hat{L}(\mathbf{\Omega}) = \hat{E}$. The inverse operator $\hat{L}^{-1}(\mathbf{\Omega})$ is given by

$$\hat{L}^{-1}(\mathbf{\Omega}) \equiv L^{-1}_{ijmn}(\mathbf{\Omega}) = \frac{1}{2}[B_1\delta_{im}\delta_{jn} + B_2 k_{ijmn} + B_3(\varepsilon_{ipm}\delta_{jn} + \varepsilon_{jpn}\delta_{im})\hat{k}_p + B_4(\delta_{im}k_{jn} + \delta_{jn}k_{im}) + B_5\varepsilon_{ipm}\varepsilon_{jqn}k_{pq} + B_6(\varepsilon_{ipm}k_{jpn} + \varepsilon_{jpn}k_{ipm})], \quad (B3)$$

where $B_1 = 1 + \chi(2\psi)$, $B_2 = B_1 + 2 - 4\chi(\psi)$, $B_3 = 2\psi\chi(2\psi)$, $B_4 = 2\chi(\psi) - B_1$, $B_5 = 2 - B_1$, $B_6 = 2\psi[\chi(\psi) - \chi(2\psi)]$, $\chi(x) = 1/(1+x^2)$, and $\psi = 2\tau(k)(\mathbf{k}\cdot\mathbf{\Omega})/k$.

Multiplying Eq. (B2) by the operator $\hat{E} + \tau(k)\hat{L}^{-1}(\mathbf{\Omega})\hat{I}(\tilde{\mathbf{U}})$ yields the second moment $\hat{f} \equiv f_{ij}(\mathbf{k}, \mathbf{R})$:

$$\hat{f} \approx [\hat{L}^{-1}(\mathbf{\Omega}) + \tau(k)\hat{L}^{-1}(\mathbf{\Omega})\hat{I}(\tilde{\mathbf{U}})\hat{L}^{-1}(\mathbf{\Omega})]\hat{f}^{(0)}, \quad (B4)$$

where we neglected terms which are of the order of $O(|\nabla\tilde{\mathbf{U}}|^2)$. Since $L^{-1}_{ijmn}(\mathbf{\Omega}) P_{mn}(\mathbf{k}) = P_{ij}(\mathbf{k})$, Eq. (B4) reads

$$\hat{f} \approx \hat{f}^{(0)} + \tau(k)\hat{L}^{-1}(\mathbf{\Omega})\hat{I}(\tilde{\mathbf{U}})\hat{f}^{(0)}. \quad (B5)$$

The first term in Eq. (B5) describes the background turbulence. The second term in Eq. (B5) determines effects of both rotation and mean gradients of the velocity perturbations on the turbulence. The integration in $\mathbf{k}$ space yields the second moment $\tilde{f}_{ij}(\mathbf{R}) = \int \tilde{f}_{ij}(\mathbf{k}, \mathbf{R}) d\mathbf{k}$ which is determined by Eq. (17), where we used the notation $\tilde{f} \equiv \tilde{f}_{ij} = f_{ij} - f_{ij}^{(0)}$, and the tensors M_{ij} and S_{ij} are given by

$$M_{ij} = D_1(\omega)(\partial\tilde{U})_{ij} + D_2(\omega) Q_{ij} + D_3(\omega) T_{ij} + D_4(\omega)(\hat{\boldsymbol{\omega}}\cdot\boldsymbol{\nabla}) \times (\hat{\boldsymbol{\omega}}\cdot\tilde{\mathbf{U}})\omega_{ij}, \quad (B6)$$

$$S_{ij} = D_5(\omega) K_{ij} + D_6(\omega) R_{ij}, \quad (B7)$$

where

$$Q_{ij} = (\hat{\omega}_i\nabla_j + \hat{\omega}_j\nabla_i)(\hat{\boldsymbol{\omega}}\cdot\tilde{\mathbf{U}}) + (\hat{\boldsymbol{\omega}}\cdot\boldsymbol{\nabla})(\hat{\omega}_i\tilde{U}_j + \hat{\omega}_j\tilde{U}_i), \quad (B8)$$

$$T_{ij} = (\hat{\boldsymbol{\omega}}\times\boldsymbol{\nabla})_i(\hat{\boldsymbol{\omega}}\times\tilde{\mathbf{U}})_j + (\hat{\boldsymbol{\omega}}\times\boldsymbol{\nabla})_j(\hat{\boldsymbol{\omega}}\times\tilde{\mathbf{U}})_i, \quad (B9)$$

$$K_{ij} = \hat{\omega}_n[\varepsilon_{imn}(\partial\tilde{U})_{mj} + \varepsilon_{jmn}(\partial\tilde{U})_{mi}], \quad (B10)$$

$$R_{ij} = [\hat{\omega}_i(\hat{\boldsymbol{\omega}}\times\boldsymbol{\nabla})_j + \hat{\omega}_j(\hat{\boldsymbol{\omega}}\times\boldsymbol{\nabla})_i](\hat{\boldsymbol{\omega}}\cdot\tilde{\mathbf{U}}) + (\hat{\boldsymbol{\omega}}\cdot\boldsymbol{\nabla})[\hat{\omega}_i(\hat{\boldsymbol{\omega}}\times\tilde{\mathbf{U}})_j + \hat{\omega}_j(\hat{\boldsymbol{\omega}}\times\tilde{\mathbf{U}})_i], \quad (B11)$$

$(\partial\tilde{U})_{ij} = (\nabla_i\tilde{U}_j + \nabla_j\tilde{U}_i)/2$, $\omega_{ij} = \hat{\omega}_i\hat{\omega}_j$, $\hat{\omega}_i = \Omega_i/\Omega$, and

$$D_1(\omega) = \{2[A_1^{(1)}(\omega) - A_1^{(1)}(0) + (q+2)C_1^{(1)}(0) + C_1^{(1)}(\omega)] + A_2^{(1)}(\omega)\}/4,$$

$$D_2(\omega) = [2C_3^{(1)}(\omega) - A_2^{(1)}(\omega)]/8,$$

$$D_3(\omega) = -(1/8)A_2^{(1)}(\omega), \quad D_4(\omega) = (1/4)C_2^{(1)}(\omega),$$

$$D_5(\omega) = 2[4C_1^{(2)}(\omega) + C_2^{(2)}(\omega) + 7C_3^{(2)}(\omega)],$$

$$D_6(\omega) = C_2^{(2)}(\omega) + 2C_3^{(2)}(\omega),$$

$\omega = 8\tau_0\Omega$. The functions $A_m^{(n)}(\omega)$ and $C_m^{(n)}(\omega)$ are determined in Appendix C. Equation (18) for the effective force $\tilde{\boldsymbol{\mathcal{F}}} = -\nabla_j\tilde{f}_{ij}(\mathbf{R})$ can be rewritten in the form

$$\tilde{\mathcal{F}}_i = \tilde{\mathcal{F}}_i^{(H)} + \left(\nu_T^{(0)} M_{ij} + \frac{1}{6} l_0^2 \Omega S_{ij}\right)\Lambda_j, \tag{B12}$$

where $\nu_T^{(0)} = \tau_0 \langle \mathbf{u}^2 \rangle^{(0)}/6 = l_0^2/6\tau_0$, $\boldsymbol{\Lambda} = (\boldsymbol{\nabla} l_0^2)/l_0^2 = (\boldsymbol{\nabla}\nu_T^{(0)})/\nu_T^{(0)}$, and the effective force $\tilde{\mathcal{F}}_i^{(H)}$ in a homogeneous turbulence reads

$$\begin{aligned}\tilde{\mathcal{F}}_i^{(H)} = \nu_T^{(0)}\Bigg\{ \left[\frac{1}{2}D_1 - D_3\right]\Delta \tilde{U}_i + D_4 \hat{\omega}_i (\hat{\boldsymbol{\omega}}\cdot\boldsymbol{\nabla})^2(\hat{\boldsymbol{\omega}}\cdot\tilde{\mathbf{U}}) \\ + (D_2 + D_3)[(\hat{\boldsymbol{\omega}}\cdot\boldsymbol{\nabla})^2\tilde{U}_i + \hat{\omega}_i\Delta(\hat{\boldsymbol{\omega}}\cdot\tilde{\mathbf{U}})]\Bigg\} \\ + \frac{1}{6}l_0^2\Omega\Bigg[D_6(\hat{\boldsymbol{\omega}}\cdot\boldsymbol{\nabla})[(\hat{\boldsymbol{\omega}}\times\boldsymbol{\nabla})_i(\hat{\boldsymbol{\omega}}\cdot\tilde{\mathbf{U}}) - (\hat{\boldsymbol{\omega}}\cdot\tilde{\mathbf{W}})\omega_i \\ + (\hat{\boldsymbol{\omega}}\cdot\boldsymbol{\nabla})(\hat{\boldsymbol{\omega}}\times\tilde{\mathbf{U}})_i] - \frac{1}{2}D_5\Delta(\hat{\boldsymbol{\omega}}\times\tilde{\mathbf{U}})_i\Bigg] \\ + \frac{1}{12}l_0^2\Omega D_5\nabla_i(\hat{\boldsymbol{\omega}}\cdot\tilde{\mathbf{W}}) + \nu_T^{(0)}(D_2 - D_3)\nabla_i(\hat{\boldsymbol{\omega}}\cdot\boldsymbol{\nabla}) \\ \times(\hat{\boldsymbol{\omega}}\cdot\tilde{\mathbf{U}}),\end{aligned} \tag{B13}$$

where we used the identity

$$\begin{aligned}\varepsilon_{ijk}\varepsilon_{lmn} = \delta_{il}\delta_{jm}\delta_{kn} + \delta_{in}\delta_{jl}\delta_{km} + \delta_{im}\delta_{jn}\delta_{kl} - \delta_{in}\delta_{jm}\delta_{kl} \\ - \delta_{il}\delta_{jn}\delta_{km} - \delta_{im}\delta_{jl}\delta_{kn}.\end{aligned}$$

Equation (B13) for the effective force $\tilde{\mathcal{F}}_i^{(H)}$ in a homogeneous turbulence coincides in the form with that obtained in [49] using symmetry arguments. However, the symmetry arguments cannot allow to determine the coefficients in Eq. (B13).

APPENDIX C: THE IDENTITIES USED FOR THE INTEGRATION IN k SPACE

To integrate over the angles in **k** space we used the following identities:

$$\bar{J}_{ij}(a) = \int \frac{k_{ij}\sin\theta}{1 + a\cos^2\theta} d\theta d\varphi = \bar{A}_1\delta_{ij} + \bar{A}_2\omega_{ij}, \tag{C1}$$

$$\begin{aligned}\bar{J}_{ijmn}(a) = \int \frac{k_{ijmn}\sin\theta}{1 + a\cos^2\theta} d\theta d\varphi = \bar{C}_1(\delta_{ij}\delta_{mn} + \delta_{im}\delta_{jn} + \delta_{in}\delta_{jm}) \\ + \bar{C}_2\omega_{ijmn} + \bar{C}_3(\delta_{ij}\omega_{mn} + \delta_{im}\omega_{jn} + \delta_{in}\omega_{jm} + \delta_{jm}\omega_{in} \\ + \delta_{jn}\omega_{im} + \delta_{mn}\omega_{ij}),\end{aligned} \tag{C2}$$

$$\begin{aligned}\bar{H}_{ijmn}(a) &= \int \frac{k_{ijmn}\sin\theta}{(1 + a\cos^2\theta)^2} d\theta d\varphi \\ &= -\left(\frac{\partial}{\partial b}\int \frac{k_{ijmn}\sin\theta}{b + a\cos^2\theta} d\theta d\varphi\right)_{b=1} \\ &= \bar{J}_{ijmn}(a) + a\frac{\partial}{\partial a}\bar{J}_{ijmn}(a),\end{aligned} \tag{C3}$$

where $\omega_{ij} = \hat{\omega}_i\hat{\omega}_j$, $\omega_{ijmn} = \omega_{ij}\omega_{mn}$, $\bar{A}_1 = 5\bar{C}_1 + \bar{C}_3$, $\bar{A}_2 = \bar{C}_2 + 7\bar{C}_3$, and

$$\bar{A}_1(a) = \frac{2\pi}{a}\left[(a+1)\frac{\arctan(\sqrt{a})}{\sqrt{a}} - 1\right],$$

$$\bar{A}_2(a) = -\frac{2\pi}{a}\left[(a+3)\frac{\arctan(\sqrt{a})}{\sqrt{a}} - 3\right],$$

$$\bar{C}_1(a) = \frac{\pi}{2a^2}\left[(a+1)^2\frac{\arctan(\sqrt{a})}{\sqrt{a}} - \frac{5a}{3} - 1\right],$$

$$\bar{C}_2(a) = \frac{\pi}{2a^2}\left[(3a^2 + 30a + 35)\frac{\arctan(\sqrt{a})}{\sqrt{a}} - \frac{55a}{3} - 35\right],$$

$$\bar{C}_3(a) = -\frac{\pi}{2a^2}\left[(a^2 + 6a + 5)\frac{\arctan(\sqrt{a})}{\sqrt{a}} - \frac{13a}{3} - 5\right].$$

In the case of $a \ll 1$ these functions are given by

$$\bar{A}_1(a) \sim (4\pi/3)[1 - (1/5)a], \quad \bar{A}_2(a) \sim -(8\pi/15)a,$$

$$\bar{C}_1(a) \sim (4\pi/15)[1 - (1/7)a], \quad \bar{C}_2(a) \sim (32\pi/315)a^2,$$

$$\bar{C}_3(a) \sim -(8\pi/105)a.$$

In the case of $a \gg 1$ these functions are given by

$$\bar{A}_1(a) \sim \pi^2/\sqrt{a}, \quad \bar{A}_2(a) \sim -\pi^2/\sqrt{a},$$

$$\bar{C}_1(a) \sim \pi^2/4\sqrt{a} - 4\pi/3a, \quad \bar{C}_2(a) \sim 3\pi^2/4\sqrt{a},$$

$$\bar{C}_3(a) \sim -\pi^2/4\sqrt{a} + 8\pi/3a.$$

Now we calculate the functions

$$A_k^{(p)}(\omega) = (6/\pi\omega^{p+1})\int_0^\omega y^p \bar{A}_k(y^2)dy,$$

$$C_k^{(p)}(\omega) = (6/\pi\omega^{p+1})\int_0^\omega y^p \bar{C}_k(y^2)dy.$$

The integration yields

$$A_1^{(1)}(\omega) = 12\left[\frac{\arctan(\omega)}{\omega}\left(1 - \frac{1}{\omega^2}\right) + \frac{1}{\omega^2}[1 - \ln(1+\omega^2)]\right],$$

$$A_2^{(1)}(\omega) = -12\left[\frac{\arctan(\omega)}{\omega}\left(1 - \frac{3}{\omega^2}\right) + \frac{1}{\omega^2}[3 - 2\ln(1+\omega^2)]\right],$$

$$\begin{aligned}C_1^{(1)}(\omega) = \frac{\arctan(\omega)}{\omega}\left(3 - \frac{6}{\omega^2} - \frac{1}{\omega^4}\right) \\ + \frac{1}{\omega^2}\left(\frac{17}{3} + \frac{1}{\omega^2} - 4\ln(1+\omega^2)\right),\end{aligned}$$

$$A_1^{(2)}(\omega) = 6\left[\frac{\arctan(\omega)}{\omega}\left(1 + \frac{1}{\omega^2}\right) - \frac{3}{\omega^2} + \frac{2}{\omega^3}S(\omega)\right],$$

$$A_2^{(2)}(\omega) = -6\left[\frac{\arctan(\omega)}{\omega}\left(1+\frac{1}{\omega^2}\right) - \frac{7}{\omega^2} + \frac{6}{\omega^3}S(\omega)\right],$$

$$C_1^{(2)}(\omega) = (3/2)\left[\frac{\arctan(\omega)}{\omega}\left(1-\frac{1}{\omega^4}\right) - \frac{13}{3\omega^2} + \frac{1}{\omega^4} + \frac{4}{\omega^3}S(\omega)\right],$$

$$C_2^{(p)}(\omega) = A_2^{(p)}(\omega) - 7A_1^{(p)}(\omega) + 35C_1^{(p)}(\omega),$$

$$C_3^{(p)}(\omega) = A_1^{(p)}(\omega) - 5C_1^{(p)}(\omega),$$

where $S(\omega)=\int_0^\omega[\arctan(y)/y]dy$. In the case of $\omega \ll 1$ these functions are given by

$$A_1^{(1)}(\omega) \sim 4\left(1-\frac{1}{10}\omega^2\right), \quad A_2^{(1)}(\omega) \sim -\frac{4}{5}\omega^2,$$

$$A_1^{(2)}(\omega) \sim \frac{8}{3}\left(1-\frac{3}{25}\omega^2\right), \quad A_2^{(2)}(\omega) \sim -\frac{16}{25}\omega^2,$$

$$C_1^{(1)}(\omega) \sim \frac{4}{5}\left(1-\frac{1}{14}\omega^2\right), \quad C_2^{(1)}(\omega) \sim O(\omega^4),$$

$$C_3^{(1)}(\omega) \sim -\frac{4}{35}\omega^2, \quad C_1^{(2)}(\omega) \sim \frac{8}{15}\left(1-\frac{3}{35}\omega^2\right),$$

$$C_2^{(2)}(\omega) \sim O(\omega^4), \quad C_3^{(2)}(\omega) \sim -\frac{16}{175}\omega^2.$$

[1] J. Pedlosky, *Geophysical Fluid Dynamics* (Springer, New York, 1987), and references therein.
[2] H. P. Greenspan, *The Theory of Rotating Fluids* (Breukelen Press, Brookline, 1990), and references therein.
[3] J. H. Shirley and R. W. Fairbridge, *Encyclopedia of Planetary Sciences* (Kluwer Academic, Dordrecht, 1997), and references therein.
[4] S. S. Moiseev, R. Z. Sagdeev, A. V. Tur, G. A. Khomenko, and A. M. Shukurov, Dokl. Akad. Nauk SSSR **273**, 549 (1983) [Sov. Phys. Dokl. **28**, 925 (1983)].
[5] U. Frisch, Z. S. She, and P. L. Sulem, Physica D **28**, 382 (1987).
[6] G. A. Khomenko, S. S. Moiseev, and A. V. Tur, J. Fluid Mech. **225**, 355 (1991).
[7] O. G. Chkhetiany, S. S. Moiseev, A. S. Petrosyan, and R. Z. Sagdeev, Phys. Scr. **49**, 214 (1994).
[8] L. L. Kitchatinov, G. Rüdiger, and G. Khomenko, Astron. Astrophys. **287**, 320 (1994).
[9] A. D. McEwan, Geophys. Fluid Dyn. **5**, 283 (1973); Nature (London) **260**, 126 (1976).
[10] E. J. Hopfinger, F. K. Browand, and A. Gagne, J. Fluid Mech. **125**, 505 (1982).
[11] X. Zhang, D. L. Boyer, and H. J. S. Fernando, J. Fluid Mech. **350**, 97 (1997).
[12] M. Tanaka, S. Yanase, S. Kida, and G. Kawahara, Flow, Turbul. Combust. **60**, 301 (1998).
[13] D. M. Mason and R. R. Kerswell, J. Fluid Mech. **396**, 73 (1999).
[14] F. S. Godeferd and L. Lollini, J. Fluid Mech. **393**, 257 (1999).
[15] S. V. Alekseenko, P. A. Kuibin, V. L. Okulov, and S. I. Shtork, J. Fluid Mech. **382**, 195 (1999).
[16] F. P. Bretherton and J. S. Turner, J. Fluid Mech. **32**, 449 (1968).
[17] D. O. Gough and D. Linden-Bell, J. Fluid Mech. **32**, 437 (1968).
[18] T. Elperin, N. Kleeorin, and I. Rogachevskii, Phys. Rev. E **68**, 016311 (2003).
[19] L. Prandtl, *Essentials of Fluid Dynamics* (Blackie, London, 1952).
[20] A. A. Townsend, *The Structure of Turbulent Shear Flow* (Cambridge University Press, Cambridge, England, 1956).
[21] P. Bradshaw, Annu. Rev. Fluid Mech. **19**, 53 (1987), and references therein.
[22] A. J. Chorin, *Vorticity and Turbulence* (Springer, New York, 1994), and references therein.
[23] F. H. Busse and R. Simitev, J. Fluid Mech. **498**, 23 (2004).
[24] C. Cambon and J. F. Scott, Annu. Rev. Fluid Mech. **31**, 1 (1999).
[25] C. N. Baroud, B. B. Plapp, H. L. Swinney, and Z.-S. She, Phys. Fluids **15**, 2091 (2003).
[26] S. Galtier, Phys. Rev. E **68**, 015301(R) (2003).
[27] C. Cambon, R. Rubinstein, and F. S. Godeferd, New J. Phys. **6**, 73 (2004).
[28] A. D. Wheelon, Phys. Rev. **105**, 1706 (1957).
[29] G. K. Batchelor, I. D. Howells, and A. A. Townsend, J. Fluid Mech. **5**, 134 (1959).
[30] G. S. Golitsyn, Dokl. Akad. Nauk **132**, 315 (1960) [Sov. Phys. Dokl. **5**, 536 (1960)].
[31] H. K. Moffatt, J. Fluid Mech. **11**, 625 (1961).
[32] J. L. Lumley, Phys. Fluids **10**, 1405 (1967).
[33] J. C. Wyngaard and O. R. Cote, Q. J. R. Meteorol. Soc. **98**, 590 (1972).
[34] S. G. Saddoughi and S. V. Veeravalli, J. Fluid Mech. **268**, 333 (1994).
[35] T. Ishihara, K. Yoshida, and Y. Kaneda, Phys. Rev. Lett. **88**, 154501 (2002).
[36] T. Elperin, N. Kleeorin, I. Rogachevskii, and S. S. Zilitinkevich, Phys. Rev. E **66**, 066305 (2002).
[37] S. A. Orszag, J. Fluid Mech. **41**, 363 (1970), and references therein.
[38] A. S. Monin and A. M. Yaglom, *Statistical Fluid Mechanics* (MIT Press, Cambridge, MA, 1975), and references therein.
[39] W. D. McComb, *The Physics of Fluid Turbulence* (Clarendon, Oxford, 1990).
[40] A. Pouquet, U. Frisch, and J. Leorat, J. Fluid Mech. **77**, 321 (1976).
[41] N. Kleeorin, I. Rogachevskii, and A. Ruzmaikin, Sov. Phys. JETP **70**, 878 (1990); N. Kleeorin, M. Mond, and I. Ro-

gachevskii, Astron. Astrophys. **307**, 293 (1996).
[42] I. Rogachevskii and N. Kleeorin, Phys. Rev. E **61**, 5202 (2000); **64**, 056307 (2001); **68**, 036301 (2003); **70**, 046310 (2004).
[43] A. Brandenburg, P. Käpylä, and A. Mohammed, Phys. Fluids **16**, 1020 (2004).
[44] T. Elperin, N. Kleeorin, and I. Rogachevskii, Phys. Rev. E **52**, 2617 (1995).
[45] H. K. Moffatt, *Magnetic Field Generation in Electrically Conducting Fluids* (Cambridge University Press, New York, 1978).
[46] A. Ruzmaikin, A. M. Shukurov, and D. D. Sokoloff, *Magnetic Fields of Galaxies* (Kluwer Academic, Dordrecht, 1988).
[47] P. N. Roberts and A. M. Soward, Astron. Nachr. **296**, 49 (1975).
[48] N. Kleeorin and I. Rogachevskii, Phys. Rev. E **50**, 2716 (1994).
[49] J. Gaite, Phys. Rev. E **68**, 056310 (2003).
[50] L. Facciolo and P. H. Alfredsson, Phys. Fluids **16**, L71 (2004).